ARTICLE

Straightforward and regiospecific synthesis of 1,3,5,7-tetra-arylated acene bearing different aryl groups

Received 00th January 20xx,
Accepted 00th January 20xx

DOI: 10.1039/x0xx00000x

www.rsc.org/

Ryota Sato,[a] Kunfeng Chen[a], Takeshi Yasuda,[b] Takaki Kanbara,*[a] and Junpei Kuwabara*[a]

Multiple arylated acene derivatives play an important role in organic electronic materials. In this study, we developed a protocol for the synthesis of 1,3,5,7-tetra-arylated acenes by combining conventional cross-coupling and unique regio-selective cross-dehydrogenative coupling (CDC) reactions. 1,3,5,7-Tetra-arylated acene derivatives with different aryl groups were synthesised by first introducing aryl groups at the 1,5-positions via conventional cross-coupling reactions and then selectively introducing pentafluorophenyl groups at the sterically favourable 3,7-positions via CDC reactions. The CDC reactions proceeded smoothly on the substrates with moderately electron-donating substituents at the 1,5-positions. The crystal structure and basic physical properties of the products were elucidated, and one of 1,3,5,7-tetra-arylated anthracenes was found to function as a light-emitting material in organic light-emitting diodes.

Introduction

Multiple-arylated acenes (MAAs), in which multiple aryl groups are introduced into acenes, are promising molecules with potential applications in organic electronic materials. [1–10] MAAs, such as 2,6-diphenylanthracene[11,12] and rubrene,[9,10] have high carrier mobility due to their rigid backbone and stability due to extended π-conjugation through single bonds.[13] The development of MAAs can be accelerated by establishing an efficient synthetic method that allows for the introduction of aryl groups more conveniently and precisely. A reasonable and easy method to synthesise MAAs is the C–H direct functionalization of acene. Recently, we reported a Pd-catalysed cross-dehydrogenative coupling (CDC) reaction for the synthesis of MAAs containing two polyfluoroarene groups (Scheme 1a).[14] This reaction proceeds at the sterically vacant positions (2,6,7) of acene, in contrast to the general regioselectivity of Pd-catalysed C–H functionalization at the 1-position.[15–20] However, the regioselective control of the second polyfluoroarylation is a synthetic challenge, and the reaction leads to a mixture of 2,6 and 2,7-arylated anthracenes. In addition, this reaction cannot introduce more than two polyfluoroaryl groups. Kobayashi et al. successfully introduced four aryl groups into anthracene to obtain 1,3,5,7-tetra-arylated anthracene derivatives (TAAnts, Scheme 1b).[21] After Ir-catalysed C–H borylation of unsubstituted anthracene, the 1,3,5,7-substituted compound was isolated from a mixture of regioisomers. Subsequently, four aryl groups were introduced by conventional cross-coupling reactions to synthesise the 1,3,5,7-TAAnts. Michaels et al. also synthesised 1,3,5,7-TAAnts by the reaction of *p*-diodobenzene with acetophenone in the presence of a Pd catalyst (Scheme S1).[22] These methods are excellent for the synthesis of structurally unique 1,3,5,7-TAAnts. However, it is difficult to introduce different aryl groups in a regiospecific manner. The introduction of different aryl groups into acenes is important for electronic tuning and

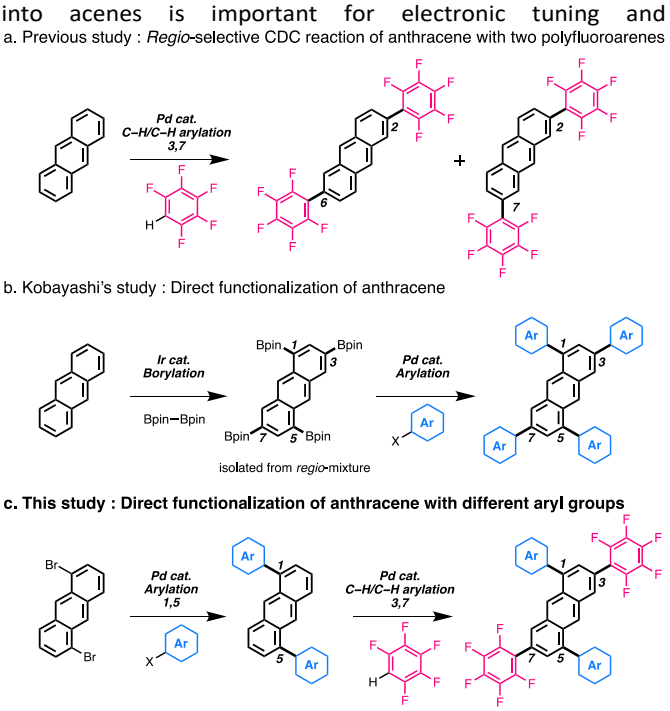

Scheme 1. Synthetic methods for multiple arylated anthracene via C—H bonds functionalization.

[a] Tsukuba Research Center for Energy Materials Science (TREMS), Institute of Pure and Applied Sciences, University of Tsukuba, 1-1-1 Tennodai, Tsukuba, Ibaraki 305-8573, Japan. E-mail: kanbara@ims.tsukuba.ac.jp kuwabara@ims.tsukuba.ac.jp
[b] Research Center for Macromolecules and Biomaterials, National Institute for Materials Science (NIMS), 1-2-1 Sengen, Tsukuba, Ibaraki 305-0047, Japan.

† Footnotes relating to the title and/or authors should appear here.
Electronic Supplementary Information (ESI) available: [details of any supplementary information available should be included here]. See DOI: 10.1039/x0xx00000x

control of molecular assemblies. For example, Okamoto et al. reported that 5-pentafluorophenyl-11-phenyltetracene forms a two-dimensional molecular assembly because of intermolecular interactions between the pentafluorophenyl and phenyl groups.[23] We hypothesised that the steric effect of the initially introduced aryl groups at the 1,5-positions would allow the regioselective introduction of aryl groups at the 3,7-positions in the second CDC reaction (Scheme 1c). In this study, we aim to prove this concept and develop a simple and precise synthetic method for the introduction of different aryl groups at the 1,5 and 3,7-positions of acenes. In addition, we have evaluated the intermolecular interactions and basic physical properties of the new acene-based materials and their potential for use as light-emitting materials in organic light-emitting diodes (OLEDs).

Results and discussion

Various 1,5-diarylnaphthalenes were synthesised by introducing substituents into easily available 1,5-dibromonaphthalene by conventional cross-coupling reactions (Scheme 2). First, *m*-xylyl groups were introduced into 1,5-dibromonaphthalene by a Suzuki-Miyaura cross-coupling reaction (Scheme 2a). Then, 1,5-bis(pentafluorophenyl)naphthalene was synthesised by direct arylation (Scheme 2b). The use of a bulky SPhos ligand[24] resulted in the formation of the desired product with an 86% yield (Table S1, Entry 3). We believe that SPhos accelerates the reductive elimination process, which is slowed down by the electron-deficient pentafluorophenyl group.[25–27] We subsequently attempted to synthesise 1,5-bis[*N,N*-bis(*m*-xylyl)amino]naphthalene by the Buchwald-Hartwig amination reaction (Scheme 2c). The reaction proceeded efficiently when XPhos ligand[28] was used (Table S2), and the target product was isolated with an 81% yield.[27] Similarly, 1,5-bis(*m*-xylyl)anthracene and 1,5-bis(pentafluorophenyl)anthracene were also synthesised (Figure 1, Scheme S2).

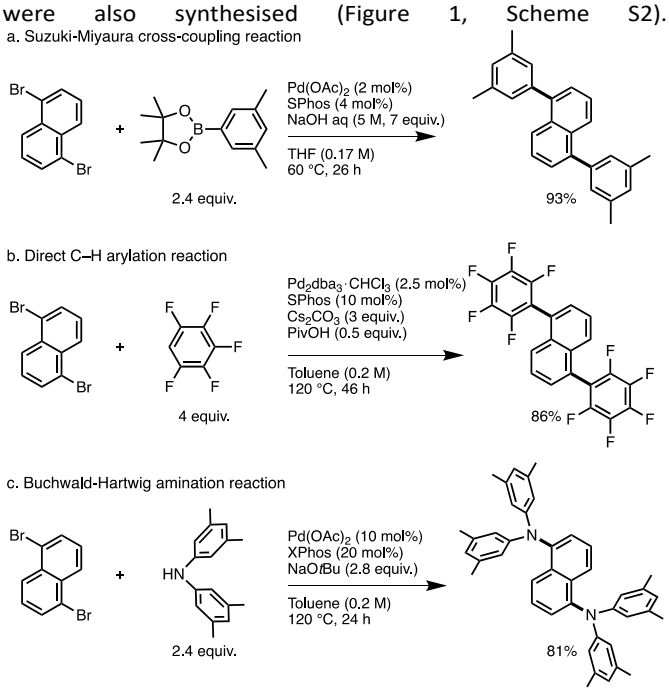

Scheme 2. Synthesis of 1,5-diarylnaphthalenes.

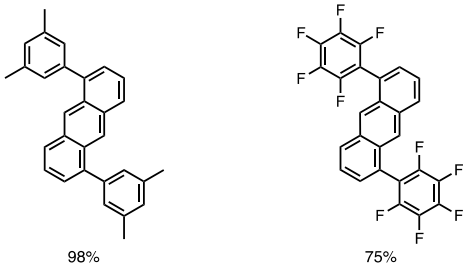

Figure 1. Synthesised 1,5-diarylanthracenes.

We optimised the conditions for the CDC reaction of 1,5-bis(*m*-xylyl)naphthalene with pentafluorobenzene (Table 1). When the reaction was performed under previously reported conditions,[14] the isolated yield was low (entry 1). Increasing the amount of catalyst and reaction time led to a 48% NMR yield of the product (entry 2). The yield was improved by increasing the reaction concentration (entry 3). Finally, the addition of a small amount of a highly polar solvent significantly improved the NMR yield (entry 4). It is known that in CDC reactions, highly polar solvents are suitable for substrates with a highly reactive C–H bond, such as thiophene,[29–31] and low-polarity solvents are suitable for substrates with low reactivity, such as naphthalene.[14] As the reactivity of the C–H bond of 1,5-bis(*m*-xylyl)naphthalene is moderate, mixed solvents would be effective for the reaction.

Table 1. Optimisation of CDC reaction conditions

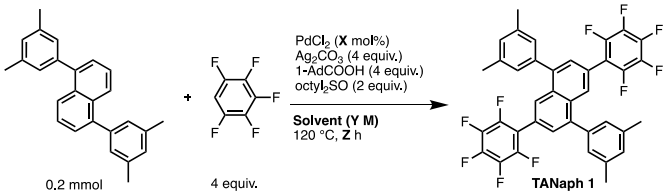

Entry	X	Solv.[b]	Y	Z	NMR yield [%][a]	Isolated yield [%]
1	10	CPME	0.25	48	-	21
2	20	CPME	0.25	72	48	-
3	20	CPME	0.4	72	59	-
4	20	CPME : DMF (4:1)	0.4	72	81	66

[a] The yield was determined by ^{19}F NMR analyses of a crude product with hexafluorobenzene as an Internal standard. [b] CPME : cyclopentyl methyl ether.

In contrast the reaction with only *N,N*-dimethylacetamide (DMAc) or *N,N*-dimethylformamide (DMF) resulted in low product yields, presumably because of their high polarity (Table S3). The target product, 1,5-bis(*m*-xylyl)-3,7-bis(pentafluorophenyl)naphthalene (**TANaph 1**), was obtained in 66% yield by column chromatography and HPLC purification. This reaction generated no homocoupling products of naphthalene or pentafluorobenzene and no regioisomers as byproducts.

We synthesised 1,3,5,7-tetrakis(pentafluorophenyl) naphthalene (**TANaph 2**) under the aforementioned optimum conditions (Table 2, entry 1). However, the isolated yield was as low as 13%. When the reaction was carried out using only CPME as the solvent, a slightly improved isolated yield of 19% of **TANaph 2** was achieved (entry 2). We believe that a low-polarity solvent, CPME, is more suitable for such a reaction involving a substituent with low-reactive C–H bonds due to the two pentafluorophenyl groups on naphthalene. Indeed, in a previous study, the presence of a pentafluorobenzene group on acenes reduced the reactivity of their C–H bonds for CDC reactions.[14]

Table 2. Synthesis of 1,3,5,7-tetrakis(pentafluorophenyl) naphthalene (**TANaph 2**)

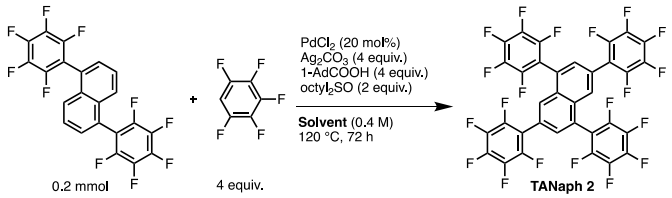

Entry	Solvent	Isolated yield [%]
1	CPME : DMF (4 : 1)	13
2	CPME	19

Subsequently, we synthesised 1,5-bis[*N,N*-bis(*m*-xylyl)amino]-3,7-bis(pentafluorophenyl)naphthalene (**TANaph 3**) (Scheme 6). The isolated yield was the lowest at 5.5%. As the 1,5-diaminonaphthalene derivative tends to oxidize to form a stable quinoid structure owing to strong electron-donating diarylamine groups,[32] oxidation of the substrate with an excess amount of Ag salt would inhibit the CDC reaction.

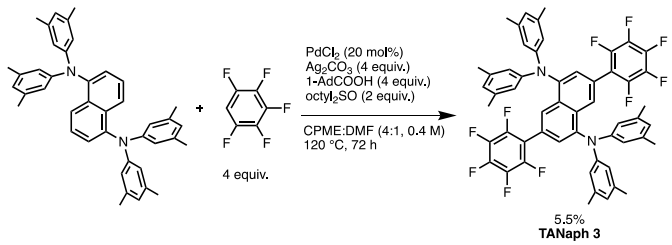

Scheme 6. Synthesis of 1,5-bis[*N,N*-di(*m*-xylyl)amino]-3,7-bis(pentafluorophenyl)naphthalene (**TANaph 3**)

Under optimised conditions, 1,5-bis(*m*-xylyl)-3,7-bis(pentafluorophenyl)anthracene (**TAAnt 1**) was obtained with a high isolated yield of 74% (Scheme 7). Similar to the synthesis of the naphthalene derivative, the yield of 1,3,5,7-tetrakis(pentafluorophenyl)anthracene (**TAAnt 2**) was low (15%), owing to the large number of pentafluorophenyl groups. **TAAnt 1** and **TAAnt 2** are readily soluble in chloroform and toluene. As the solubility is higher than that of 2,6-bis(pentafluorophenyl)naphthalene, the aromatic groups at 1 and 5 position have the effect of increasing solubility.

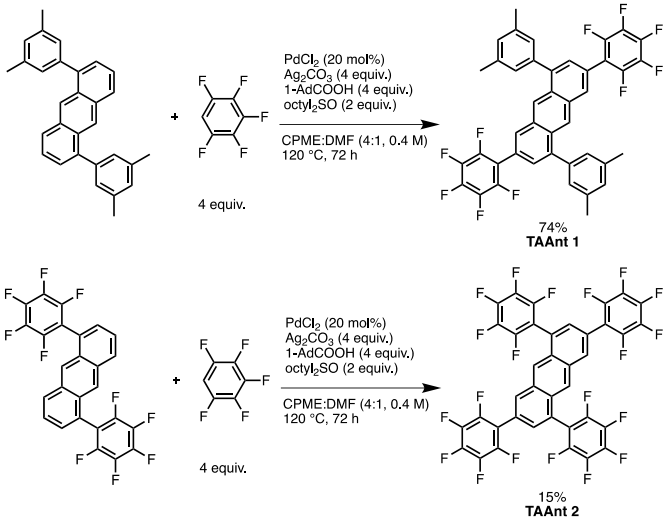

Scheme 7. Synthesis of 1,5-bis(*m*-xylyl)-3,7-bis(pentafluorophenyl)anthracene (**TAAnt 1**) and 1,3,5,7-tetrakis(pentafluorophenyl)anthracene (**TAAnt 2**).

Hence, as expected, pentafluorophenyl groups can be introduced into acenes by the CDC reaction without the formation of undesired homocoupling products or regioisomers. The pre-introduced substituents at the 1 and 5 positions provide high regioselectivity for the CDC reaction through steric effects. The electronic properties of the introduced substituents affect the reactivity of the CDC reaction. Moderately electron-donating substituents, such as *m*-xylyl groups, increase the reactivity of naphthalene and anthracene. From these results, we verify that a combination of the conventional coupling reactions and the original CDC reaction offers a new and efficient way to introduce different aryl groups into acenes in a regiospecific and straightforward manner.

The single-crystal X-ray structures of the five 1,3,5,7-tetra-arylated acenes were analyzed (Figures 2 and 3). The dihedral angles between the naphthalene core and the substituents at positions 1 and 5 are larger than those at positions 3 and 7 for all 1,3,5,7-tetra-arylated naphthalene derivatives (TANaphs). In particular, a large dihedral angle of the 1,5-pentafluorophenyl group is observed in **TANaph 2** (88°), presumably because of the steric hindrance of the fluorine groups and intermolecular interactions in the crystal packing (Figure S1). In all TANaphs, there is a long distance between the naphthalene cores, and there are no π···π interactions due to the steric repulsions of the densely introduced aryl groups.

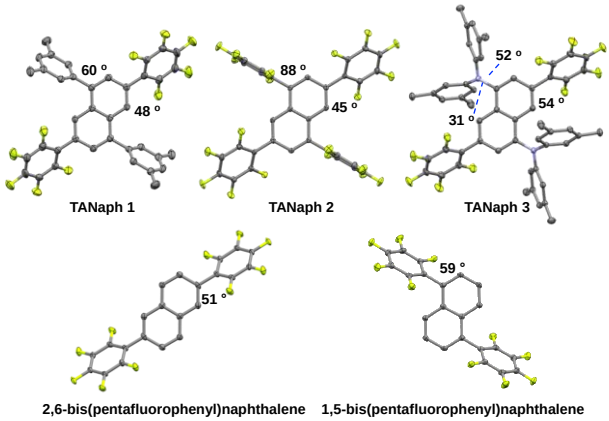

Figure 2. Single X-ray structures and dihedral angles of TANaphs and the corresponding disubstituted compounds.[14]

The single-crystal X-ray structures of the TAAnts are shown in Figure 3. The substituent dihedral angles of **TAAnt 1** are smaller than those of **TAAnt 2**, the corresponding disubstituted compounds,[8,14] and **TANaphs** (Figure 2 and S3). Additionally, π···π interactions between the anthracene cores are observed in **TAAnt 1**, possibly due to the long molecular length of anthracene, which reduces steric repulsions between the aryl substituents. The distance between the anthracene cores is 3.32 Å, which is shorter than the reported distance for anthracene derivatives (Figure 4).[33–35] Intermolecular interactions between the pentafluorophenyl and *m*-xylyl groups would contribute to the short distance between the anthracene cores. The shortest C–C distance between the pentafluorophenyl and *m*-xylyl groups is 3.34 Å, which is shorter than that (3.36 Å) observed in the co-crystal of benzene-d_6 and hexafluorobenzene,[36] as well as the molecule reported by Okamoto et al.[23] The stacked structure of **TAAnt 1** continues in a one-dimensional direction (Figure S2). The precise introduction of both electron-rich and electron-poor aryl groups enables the close assembly of acene molecules owing to multipoint interactions, which can be a supramolecular motif for assembling acenes. In contrast, **TAAnt 2**, which bears only pentafluorophenyl groups, shows no such assembled structures.

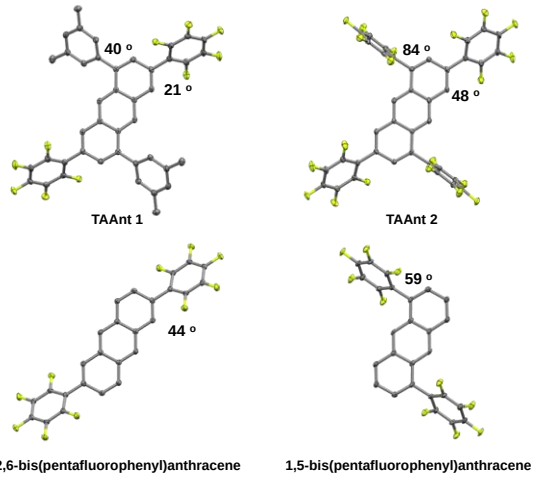

Figure 3. Single X-ray structures and dihedral angles of TAAnts and the corresponding disubstituted compounds.[8,14]

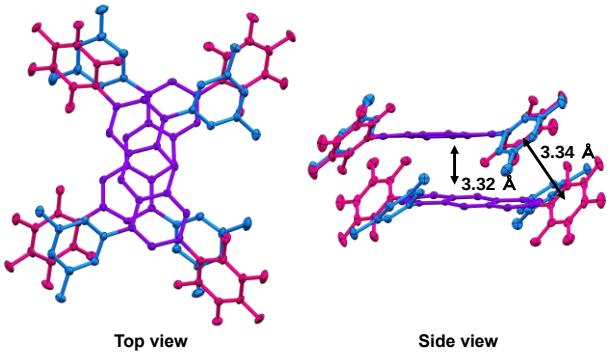

Figure 4. Assembled dimer structure of **TAAnt 1**.

TANaph 1 and **2** exhibit strong absorption peaks in the 250–270 nm region and a weak absorption peak at approximately 300 nm in solution (Table 3, Figure 5). In contrast, **TANaph 3** exhibits absorption peaks at 292 nm and 408 nm. This trend is also observed in the emission spectrum, where **TANaph 3** shows a maximum emission peak at longer wavelengths than **TANaph 1** and **2**. **TANaph 3** has strong donor and acceptor substituents, resulting in donor-acceptor transitions in the long-wavelength region.[37] Density functional theory (DFT) calculations show that the highest occupied molecular orbital (HOMO) is distributed in the donor unit and the lowest unoccupied molecular orbital (LUMO) is distributed in the acceptor unit (Figure S3). **TANaph 3** shows the highest photoluminescence quantum yield (PLQY) presumably due to the two amino groups.[38] Compared to the parent disubstituted compound, each TANaph shows long-wavelength emission (Figure S4). The appearance of solvatochromism in the emission spectrum of **TANaph 3** indicates that the transition in **TANaph 3** is charge-transfer type (Figure S5).

Table 3. Optical properties of TANaphs in chloroform solution (1.0×10^{-5} M)

Molecule	λ_{abs} [nm]	λ_{Em} [nm][a]	PLQY [%]	Lifetime [ns]
TANaph 1	264, 311	397	34	2.0
TANaph 2	259, 305	363	18	- [b]
TANaph 3	292, 408	501	53	13.7

[a] Excited at λ_{abs} (264, 259, and 292 nm). [b] not measured.

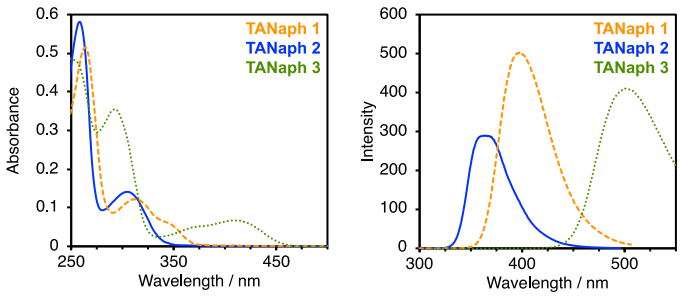

Figure 5. UV–vis absorption (left) and emission (right) spectra of TANaphs (chloroform, 1.0×10^{-5} M)

Subsequently, the optical properties of the TAAnts were evaluated (Table 4, Figure 6). In the absorption spectrum of the TAAnts, vibrational structures specific to anthracene are observed in the long-wavelength region. The absorption region of TAAnt is longer than that of the corresponding TANaph. The shapes of the absorption and emission spectra of **TAAnt 1** and **TAAnt 2** are similar, whereas **TAAnt 1** shows a slightly longer wavelength peak in both cases. The weak donor-acceptor transition is likely to be the origin of longer-wavelength absorption (Figure S6). **TAAnt 1** and **TAAnt 2** show similar PLQY and fluorescence lifetimes (Table 4).

Table 4. Optical properties of TAAnts in chloroform solution (1.0×10^{-5} M)

Molecule	λ_{abs} [nm]	λ_{Em} [nm][a]	PLQY [%]	Lifetime [ns]
TAAnt 1	289, 388	435, 458	28	2.2
TAAnt 2	287, 378	416, 439	29	2.7

[a] Excited at λ_{abs} (289 and 287 nm).

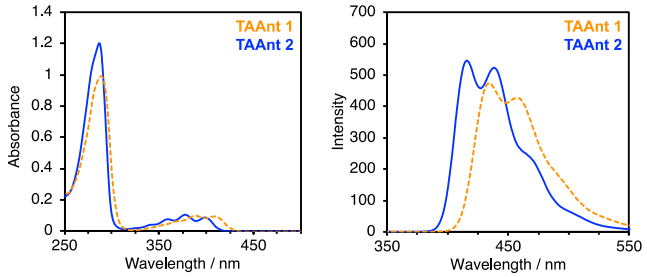

Figure 6. UV–vis absorption (left) and emission (right) spectra of TAAnts (chloroform, 1.0×10^{-5} M).

Next, we evaluated the solid-state luminescence properties of **TAAnt 1**, which exhibited unique intermolecular interactions in its crystal structure. The crystalline sample shows a sharp emission spectrum with a full width at half maximum (FWHM) of 55 nm and a maximum at 495 nm (Figure 7, Table 5, entry 1). After grinding the crystal sample, the emission peak of the powdered sample shifts slightly to shorter wavelengths and broadens (entry 2). The homogeneous stacked structure in the crystal state results in a sharper emission peak than that of the powder sample containing diverse structures.[39] We further evaluated the emission properties of the vacuum-deposited films (entry 3). The vacuum-deposited film shows significantly broadened emission in the longer wavelength region (λ_{Em} = 501 nm). The emission decay of the film at its maximum emission wavelength (501 nm) was measured. The result indicates the presence of more than three emission components. The lifetime of the main component was estimated to be 11.2 ns. Thin-film XRD and atomic force microscopy (AFM) measurements show that the vacuum-deposited film is in an amorphous state (Figure S8), which indicates disordered molecular orientations in contrast to the crystal state. Such structural diversity is thought to be the reason for the broad range of emissions. The PLQY of the vacuum-deposited film is 29%, which is almost the same as the value in the solution state.

In the film state of **TAAnt 1**, the HOMO and LUMO energy levels were obtained as -6.33 and -3.49 eV, respectively. These values are deeper than those of estimated values by DFT calculation; HOMO (-5.36 eV) and LUMO (-2.13 eV) (Figure S6). The DSC curve shows a clear melting point at 309 ºC in the second scan, which indicates thermal stability of **TAAnt 1** more than 300 ºC (Figure S9).

Table 5. Optical properties of **TAAnt 1** in solid state

Entry	State	λ_{Em} [nm][a]	FWHM [nm]
1	Crystal	495	55
2	Ground powder	477	83
3	Vacuum-deposited film	501[b]	243

[a] Exited at 380 nm, [b] exited at 400 nm.

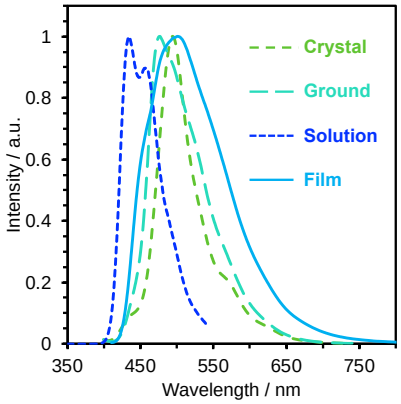

Figure 7. Emission spectra of **TAAnt 1** in the solution and solid state.

Finally, **TAAnt 1** was evaluated as a light-emitting material for OLEDs because of its amorphous nature and relatively high PLQY values (Figures 8 and S10). The maximum luminance of the device with **TAAnt 1** is 2,543 cd m^{-2} at 13.6 V, and the maximum external quantum efficiency (EQE) is 1.3% at 7.8 V. Considering that PLQY of **TAAnt 1** is 29% in the film state, the maximum EQE of OLEDs with **TAAnt 1** is estimated to be 1.45%.[40] Thus, the EQE of the OLED is close to the maximum value. The EL spectrum is similar to the photoluminescence spectrum, which shows that **TAAnt 1** functions as a light-emitting material in the OLED device (Figure 8a). The slight difference in the short-wavelength region might be caused by luminance from the 2,2',2''-(1,3,5-benzinetriyl)-tris(1-phenyl-1-H-benzimidazole) (TPBi) layer because the EL device without a TPBi layer does not show such short-wavelength emission (Figure S11).

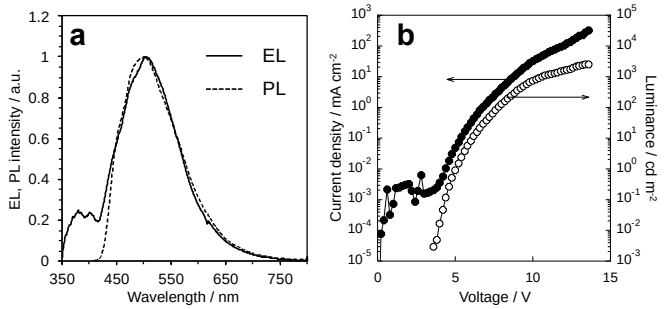

Figure 8. (a) EL spectrum of the OLED and PL spectrum of **TAAnt 1**. (b) Current density(J)-luminance(L)-voltage(V) characteristics. Device configuration: ITO/PEDOT:PSS/PVK/**TAAnt 1**/TPBi/LiF/Al.

Conclusions

In this study, we successfully synthesised 1,3,5,7-tetra-arylated acenes bearing different aryl substituents from 1,5-dibromoacene by combining a conventional cross-coupling reaction with regiospecific CDC. In the first step, aryl substituents were introduced into acenes at the 1,5-positions by conventional cross-coupling reactions. Next, the CDC reaction introduced pentafluorophenyl groups in a regiospecific manner. As undesired homo-coupling products or regioisomers were not formed, the substituents at the 1 and 5 positions provided high regioselectivity of the CDC reaction through steric effects. One of the products, 1,5-bis(*m*-xylyl)-3,7-bis(pentafluorophenyl)anthracene, formed a dense stacking structure of anthracene cores owing to multipoint interactions between *m*-xylyl and pentafluorophenyl groups. The precise introduction of both electron-rich and electron-poor aryl groups into acenes provides a new supramolecular motif for their assembly. As the developed methodology can be applied not only to acenes but also to various aromatic compounds, this method can be used to develop new materials through the precise introduction of the desired aryl groups

Author contributions

All authors contributed in varying degrees to conducting the experiments, evaluating results and writing of the manuscript; specific contributions in addition to this are listed below: R. S. performed synthesis experiments, identification and basic physical properties. and wrote the draft of the manuscript with support from J. K.. K. C. obtained data on the emission spectra and analysed them. T. Y. designed and conducted OLED experiments and obtained physical properties of the compounds in thin-film state. T. K. supervised the project and gave critical assessment throughout the progress of the project. J. K. designed the study, the main conceptual ideas, and the proof outline, and supervised the experimental work. All authors discussed the results and commented on the manuscript.

Conflicts of interest

There are no conflicts to declare.

Acknowledgements

The authors thank the Chemical Analysis Center of the University of Tsukuba for the measurements of NMR, and the single-crystal X-ray diffraction. This work was partly supported by SEI GROUP CSR Foundation, JST A-STEP Grant Number JPMJTM20BT, JPMJTM22AR, JST SPRING, Grant Number JPMJSP2124, and JSPS KAKENHI Grant Number JP22J11647, 22K05075.

References

1 T. Asako, S. Suzuki, S. Tanaka, E. Ota and J. Yamaguchi, Synthesis of Decaarylanthracene with Nine Different Substituents, *J. Org. Chem.*, 2020, **85**, 15437–15448.

2 J. E. Anthony, Functionalized Acenes and Heteroacenes for Organic Electronics, *Chem. Rev.*, 2006, **106**, 5028–5048.

3 M. Bendikov, F. Wudl and D. F. Perepichka, Tetrathiafulvalenes, Oligoacenenes, and Their Buckminsterfullerene Derivatives: The Brick and Mortar of Organic Electronics, *Chem. Rev.*, 2004, **104**, 4891–4946.

4 C. Wang, H. Dong, W. Hu, Y. Liu and D. Zhu, Semiconducting π-Conjugated Systems in Field-Effect Transistors: A Material Odyssey of Organic Electronics, *Chem. Rev.*, 2012, **112**, 2208–2267.

5 Q. Ye and C. Chi, Recent Highlights and Perspectives on Acene Based Molecules and Materials, *Chem. Mater.*, 2014, **26**, 4046–4056.

6 J. E. Anthony, The Larger Acenes: Versatile Organic Semiconductors, *Angew. Chem. Int. Ed.*, 2008, **47**, 452–483.

7 R. Liedtke, S. Surmiak, X. Jie, C. G. Daniliuc, G. Kehr and G. Erker, Ring Construction by 1,1-Carboboration; Making Anthracene Derivatives from a Tetra(alkynyl)benzene , *Helv. Chim. Acta*, 2021, **104**, e2100149.

8 R. Sato, T. Yasuda, T. Hiroto, T. Kanbara and J. Kuwabara, (in press) Facile synthesis of bis-pentafluoroarylated anthracene derivatives for n-type organic field-effect transistor applications, *Chem. Eur. J.*, DOI:10.1002/chem.202203816.

9 V. C. Sundar, E. Menard, R. L. Willett, T. Someya, M. E. Gershenson and J. A. Rogers, Elastomeric Transistor Stamps: Reversible Probing of Charge Transport in Organic Crystals, *Science*, 2004, **303**, 1644–1646.

10 T. Hasegawa and J. Takeya, Organic field-effect transistors using single crystals, *Sci. Technol. Adv. Mater.*, 2009, **10**, 024314.

11 J. Liu, H. Zhang, H. Dong, L. Meng, L. Jiang, L. Jiang, Y. Wang, J. Yu, Y. Sun, W. Hu and A. J. Heeger, High mobility emissive organic semiconductor, *Nat. Commun.*, 2015, **6**, 10032.

12 J. Liu, H. Dong, Z. Wang, D. Ji, C. Cheng, H. Geng, H. Zhang, Y. Zhen, L. Jiang, H. Fu, Z. Bo, W. Chen, Z. Shuai and W. Hu,

Thin film field-effect transistors of 2,6-diphenyl anthracene (DPA), *Chem. Commun*, 2015, **51**, 11777.

13 H. Meng, F. Sun, M. B. Goldfinger, G. D. Jaycox, Z. Li, W. J. Marshall and G. S. Blackman, High-Performance, Stable Organic Thin-Film Field-Effect Transistors Based on Bis-5'-alkylthiophen-2'-yl-2,6-anthracene Semiconductors, *J. Am. Chem. Soc.*, 2005, **127**, 2406–2407.

14 R. Sato, T. Iida, T. Kanbara and J. Kuwabara, Unique regioselectivity of the Pd-catalysed cross-dehydrogenative coupling reaction of simple polyaromatic hydrocarbons with polyfluoroarenes, *Chem. Commun.*, 2022, **58**, 11511–11514.

15 S. I. Gorelsky, D. Lapointe and K. Fagnou, Analysis of the Concerted Metalation-Deprotonation Mechanism in Palladium-Catalyzed Direct Arylation Across a Broad Range of Aromatic Substrates, *J. Am. Chem. Soc.*, 2008, **130**, 10848–10849.

16 D. Lapointe and K. Fagnou, Overview of the Mechanistic Work on the Concerted Metallation–Deprotonation Pathway, *Chem. Lett.*, 2010, **39**, 1118–1126.

17 A. Petit, J. Flygare, A. T. Miller, G. Winkel and D. H. Ess, Transition-State Metal Aryl Bond Stability Determines Regioselectivity in Palladium Acetate Mediated C–H Bond Activation of Heteroarenes, *Org. Lett.*, 2012, **14**, 3680–3683.

18 S. I. Gorelsky, D. Lapointe and K. Fagnou, Analysis of the Palladium-Catalyzed (Aromatic)C–H Bond Metalation–Deprotonation Mechanism Spanning the Entire Spectrum of Arenes, *J. Org. Chem.*, 2012, **77**, 658–668.

19 A. M. Wagner, A. J. Hickman and M. S. Sanford, Platinum-Catalyzed C–H Arylation of Simple Arenes, *J. Am. Chem. Soc.*, 2013, **135**, 15710–15713.

20 D. Kim, G. Choi, W. Kim, D. Kim, Y. K. Kang and S. H. Hong, The site-selectivity and mechanism of Pd-catalyzed C(sp^2)–H arylation of simple arenes, *Chem. Sci.*, 2021, **12**, 363–373.

21 Y. Takaki, K. Yoza and K. Kobayashi, Fourfold C–H Borylation of Anthracene: 1,3,5,7-Tetraborylanthracene and Its Application to 1,3,5,7-Tetraarylanthracenes, *Chem. Lett.*, 2017, **46**, 655–658.

22 C. C. Ence, E. E. Martinez, S. R. Himes, S. H. Nazari, M. R. Moreno, M. F. Matu, S. G. Larsen, K. J. Gassaway, G. A. Valdivia-Berroeta, S. J. Smith, D. H. Ess and D. J. Michaelis, Experiment and Theory of Bimetallic Pd-Catalyzed α-Arylation and Annulation for Naphthalene Synthesis, *ACS Catal.*, 2021, **11**, 10394–10404.

23 T. Okamoto, K. Nakahara, A. Saeki, S. Seki, J. H. Oh, H. B. Akkerman, Z. Bao and Y. Matsuo, Aryl–Perfluoroaryl Substituted Tetracene: Induction of Face-to-Face π–π Stacking and Enhancement of Charge Carrier Properties, *Chem. Mater.*, 2011, **23**, 1646–1649.

24 T. E. Barder, S. D. Walker, J. R. Martinelli and S. L. Buchwald, Catalysts for Suzuki–Miyaura Coupling Processes: Scope and Studies of the Effect of Ligand Structure, *J. Am. Chem. Soc.*, 2005, **127**, 4685–4696.

25 K. Osakada, H. Onodera and Y. Nishihara, Diarylpalladium Complexes with a Cis Structure. Formation via Transmetalation of Arylboronic Acids with an Aryliodopalladium Complex and Intramolecular Coupling of the Aryl Ligands, Affording Unsymmetrical Biaryls, *Organometallics*, 2005, **24**, 190–192.

26 V. Salamanca and A. C. Albéniz, Faster palladium-catalyzed arylation of simple arenes in the presence of a methylketone: beneficial effect of an a priori interfering solvent in C–H activation, *Org. Chem. Front.*, 2021, **8**, 1941–1951.

27 R. Martin and S. L. Buchwald, Palladium-Catalyzed Suzuki−Miyaura Cross-Coupling Reactions Employing Dialkylbiaryl Phosphine Ligands, *Acc. Chem. Res.*, 2008, **41**, 1461–1473.

28 X. Huang, K. W. Anderson, D. Zim, L. Jiang, A. Klapars and S. L. Buchwald, Expanding Pd-Catalyzed C−N Bond-Forming Processes: The First Amidation of Aryl Sulfonates, Aqueous Amination, and Complementarity with Cu-Catalyzed Reactions, *J. Am. Chem. Soc.*, 2003, **125**, 6653–6655.

29 C. Y. He, S. Fan and X. Zhang, Pd-Catalyzed Oxidative Cross-Coupling of Perfluoroarenes with Aromatic Heterocycles, *J. Am. Chem. Soc.*, 2010, **132**, 12850–12852.

30 Y. Shimoyama, J. Kuwabara and T. Kanbara, Mechanistic Study of Pd/Ag Dual-Catalyzed Cross-Dehydrogenative Coupling of Perfluoroarenes with Thiophenes, *ACS Catal.*, 2020, **10**, 3390–3397.

31 L. Xing, J. R. Liu, X. Hong, K. N. Houk and C. K. Luscombe, An Exception to the Carothers Equation Caused by the Accelerated Chain Extension in a Pd/Ag Cocatalyzed Cross Dehydrogenative Coupling Polymerization, *J. Am. Chem. Soc.*, 2022, **144**, 2311–2322.

32 P. R. Serwinski, R. Walton, J. A. Sanborn, P. M. Lahti, T. Enyo, D. Miura, H. Tomioka and A. Nicolaides, Connectivity Effects in Isomeric Naphthalenedinitrenes, *Org. Lett.*, 2001, **3**, 357–360.

33 Y. Shen, H. Liu, S. Zhang, Y. Gao, B. Li, Y. Yan, Y. Hu, L. Zhao and B. Yang, Discrete face-to-face stacking of anthracene inducing high-efficiency excimer fluorescence in solids via a thermally activated phase transition, *J. Mater. Chem. C*, 2017, **5**, 10061–10067.

34 T. Hinoue, Y. Shigenoi, M. Sugino, Y. Mizobe, I. Hisaki, M. Miyata and N. Tohnai, Regulation of π-Stacked Anthracene Arrangement for Fluorescence Modulation of Organic Solid from Monomer to Excited Oligomer Emission, *Chem. Eur. J.*, 2012, **18**, 4634–4643.

35 S. Sekiguchi, K. Kondo, Y. Sei, M. Akita and M. Yoshizawa, Engineering Stacks of V-Shaped Polyaromatic Compounds with Alkyl Chains for Enhanced Emission in the Solid State, *Angew. Chem. Int. Ed.*, 2016, **55**, 6906–6910.

36 J. H. Williams, J. K. Cockcroft and A. N. Fitch, Structure of the Lowest Temperature Phase of the Solid Benzene–Hexafluorobenzene Adduct, *Angew. Chem. Int. Ed. Engl.*, 1992, **31**, 1655–1657.

37 R. Nazir, B. Thorsted, E. Balčiunas, L. Mazur, I. Deperasińska, M. Samoć, J. Brewer, M. Farsari and D. T. Gryko, π-Expanded 1,3-diketones – synthesis, optical properties and application in two-photon polymerization, *J. Mater. Chem. C*, 2016, **4**, 167–177.

38 S. Suzuki, S. Sasaki, A. S. Sairi, R. Iwai, B. Z. Tang and G. Konishi, Principles of Aggregation-Induced Emission: Design of Deactivation Pathways for Advanced AIEgens and Applications, *Angew. Chem. Int. Ed.*, 2020, **59**, 9856–9867.

39 B. Wang, Z. Wu, B. Fang and M. Yin, Blue-shifted mechanochromism of a dimethoxynaphthalene-based crystal with aggregation-induced emission, *Dye. Pigment.*, 2020, **182**, 108618.

40 T. Tsutsui and N. Takada, Progress in Emission Efficiency of Organic Light-Emitting Diodes: Basic Understanding and Its Technical Application, *Jpn. J. Appl. Phys.*, 2013, **52**, 110001.

